author(s) details

Fate of *Trichoderma harzianum* in the olive rhizosphere: time course of the root colonization process and interaction with the fungal pathogen *Verticillium dahliae*

David Ruano-Rosa[1], Pilar Prieto[2], Ana María Rincón[3], María Victoria Gómez-Rodríguez[4], Raquel Valderrama[4], Juan Bautista Barroso[4], Jesús Mercado-Blanco[1*]

Departments of [1]Crop Protection and [2]Plant Breeding, Institute for Sustainable Agriculture, Agencia Estatal Consejo Superior de Investigaciones Científicas (CSIC), Córdoba, Spain.

[3]Department of Genetics, Faculty of Biology, University of Seville, Spain.

[4]Group of Biochemistry and Cell Signalling in Nitric Oxide, Department of Experimental Biology, Center for Advanced Studies in Olive Grove and Olive Oils, University of Jaén, Jaén, Spain.

[1] Dr. Jesús Mercado-Blanco

Institute for Sustainable Agriculture (CSIC); Department of Crop Protection;

Laboratory of Plant-Microorganism Interaction; C/ Alameda del Obispo s/n

CP 14080; Córdoba, Spain

jesus.mercado@ias.csic.es

David Ruano-Rosa is a postdoctoral researcher skilled on integrated control of soil-borne pathogens of woody plants, on the selection and characterization of biological control agents with special interest in the genera *Trichoderma* and *Pseudomonas*, and on the study of phytopathogen-biological control agent interactions.

Pilar Prieto is interested in the analysis of genome organization in cereals, particularly rice and wheat, combining confocal microscopy with genomic and proteomic approaches. The study of chromosome associations during meiosis is a relevant research topic. She aims to transfer agronomic traits into wheat by manipulating chromosome associations to promote inter-specific recombination between wheat and related species such as wild and cultivated barley. The study of the colonization processes of cereals and olive tissues by microorganisms using confocal microscopy is another research area.

Ana Rincón is researcher and lecturer at the University of Seville, Spain. Her work has been focused on molecular genetics and improvement of strains of *Trichoderma* spp. as biological control agents since 1997. She has taken part in numerous projects to develop *Trichoderma*-based formulations for crop protection.

María Victoria Gómez-Rodríguez is lecturer in plant physiology at the Universidad de Jaén, Spain, since 23 years ago. Her main research interests are plant-pathogen interaction and plant induced resistance mechanisms against oomycetes."

Raquel Valderrama is professor in Biochemistry and Molecular Biology and her investigation is focused on the study of the response of antioxidant systems and several reactive oxygen and nitrogen species (ROS and RNS) in plants during development and biotic /abiotic stress conditions.

Juan B. Barroso is full professor of Biochemistry and Molecular Biology and his research is focused on the study of the metabolism of several reactive oxygen and nitrogen species (ROS and RNS) and their implications on the plant defense mechanisms against different biotic and abiotic stress conditions.

Jesús Mercado-Blanco is tenured scientist in the Institute for Sustainable Agriculture (Spanish National Research Council, CSIC). His main research interests focus on agricultural microbiology and biotechnology and the development of control tools within integrated disease management strategies, using Verticillium wilt of olive as study model. Specific research topics are the bases underlying plant-microbe interactions by molecular and '-omic' approaches and the identification, characterization and use of microbiological control agents, with emphasis on bacterial endophytes.

Revised (blind) manuscript indicating where changes were made

1 **Fate of *Trichoderma harzianum* in the olive rhizosphere: time course of the root**
2 **colonization process and interaction with the fungal pathogen *Verticillium dahliae***
3
4 **Abstract**

5 *Trichoderma harzianum* Rifai is a well-known biological control agent (BCA) effective
6 against a wide range of phytopathogens. Since colonization and persistence in the target
7 niche is crucial for biocontrol effectiveness we aimed to: (i) shed light on the olive roots
8 colonization process by *T. harzianum* CECT 2413, (ii) unravel the fate of its biomass
9 upon application; and (iii) study the *in planta* interaction with the soil-borne pathogen
10 *Verticillium dahliae* Kleb. Fluorescently-tagged derivatives of CECT 2413 and *V.*
11 *dahliae* and confocal laser scanning microscopy were used. *In vitro* assays showed for
12 the first time mycoparasitism of *V. dahliae* by *T. harzianum*, evidenced by events such
13 as hyphal coiling. *In planta* assays revealed that CECT 2413 profusely colonized the
14 rhizoplane of olive roots. Interestingly, biomass of the BCA was visualized mainly as
15 chlamydospores. This observation was independent on the presence or absence of the
16 pathogen. Evidence of inner colonization of olive roots by CECT 2413 was not
17 obtained. These results suggest that CECT 2413 is not able to persist in a metabolically-
18 active form when applied as a spore suspension. This may have strong implications in
19 the way this BCA should be introduced and/or formulated to be effective against
20 Verticillium wilt of olive.
21

22 **Keywords**
23 Chlamydospores, Confocal laser scanning microscopy, Mycoparasitism, *Olea europaea*
24 L., *Trichoderma harzianum* Rifai, Root colonization, *Verticillium dahliae* Kleb.,
25 Verticillium wilt.

26 **Introduction**

27 A growing social demand for agricultural products free of harmful compounds for both
28 human and animal health and for the environment has encouraged the research on
29 biological control agents (BCA) as an alternative to chemical-based products for
30 effective crop diseases management. Among microorganisms studied and employed as
31 BCA, species of the filamentous fungal genus *Trichoderma* arise as one of the most
32 outstanding. *Trichoderma* spp. are thus considered the BCA par excellence among fungi
33 due to: i) their well-documented antimicrobial activity, consequence of mechanisms
34 (not mutually exclusive) such as antibiosis, mycoparasitism and/or competition
35 (Harman and Kubicek 1998; Verma et al. 2007); ii) their ability to induce systemic
36 resistance (Harman et al. 2004; Contreras-Cornejo et al. 2013); and/or iii) their positive
37 effects on seed germination and plant growth (e.g. Hermosa et al. 2012). Moreover,
38 *Trichoderma* spp. are highly versatile and show cosmopolitan distribution (Druzhinina
39 et al. 2011; Kredick et al. 2014). Taking into account all these characteristics,
40 *Trichoderma* spp. are widely selected as BCA against soil-borne pathogens (e.g. Ruano-
41 Rosa et al. 2010; 2014), and constitute the base of many registered bioformulations
42 worldwide (Verma et al. 2007; Lorito and Woo 2015). Even though our knowledge on
43 mechanisms underlying biocontrol exerted by *Trichoderma* spp. is abundant, there is
44 still an important lack of information on how *Trichoderma* spp. interact with the host
45 plant and the target phytopathogen in a scenario such as the rhizosphere, where multiple
46 trophic interactions take place (Raaijmakers et al. 2009). Research pursuing this aim is
47 scant and therefore needed to better understand the fate of this BCA once applied to
48 roots or soil, especially in the case of woody plants with large root systems.

49 *Trichoderma harzianum* Rifai is employed as BCA against a wide range of plant
50 pathogens, such as *Fusarium oxysporum* f. sp. *phaseoli* (Carvalho et al. 2014).

51 *Trichoderma harzianum* CECT 2413 is a well-documented isolate of this genus due to
52 its demonstrated mycoparasitic activity against different pathogens, for instance
53 *Rhizoctonia meloni* and *Phytophthora citrophthora* (Moreno-Mateos et al. 2007), and
54 its plant growth promotion capability (Chacón et al. 2007). Related to root colonization,
55 CECT 2413 has mostly been studied on non-woody plants like tomato (*Solanum*
56 *lycopersicum* L.) (Chacón et al. 2007), cucumber (*Cucumis sativus* L.) (Samolski et al.
57 2012) or *Arabidopsis thaliana* L. (Alonso-Ramírez et al. 2014).

58 Verticillium wilt of olive (*Olea europaea* L.) (VWO) is caused by the soil-borne
59 fungus *Verticillium dahliae* Kleb. This disease is considered one of the most important
60 biotic constraints for olive cultivation in many regions, particularly in the
61 Mediterranean Basin. Unfortunately, VWO is very difficult to control and must be
62 confronted by means of an integrated disease management (IDM) strategy (López-
63 Escudero and Mercado-Blanco 2011). An interesting approach to control VWO in a
64 sustainable, environmentally-friendly way and within IDM frameworks is by using
65 BCA, particularly at the nursery production stage (Tjamos 1993). So far, however, only
66 a few reports have demonstrated the effectiveness of BCA against VWO (Mercado-
67 Blanco et al. 2004; Prieto et al. 2009), identified a number of taxa with potential to
68 control *V. dahliae* (Papasotiriou et al. 2013), or used promising combinations of BCA
69 and organic amendments (Vitullo et al. 2013). *Trichoderma* spp. have also been
70 investigated either on their potential to antagonize *V. dahliae* in nurseries potting mixes
71 (Aleandri et al. 2015), or as bioformulations against VWO caused by the defoliating (D)
72 pathotype of *V. dahliae* (Jiménez-Díaz et al. 2009). Recently, the use of a formulation
73 based on *T. harzianum* CECT 2413 to control VWO has been patented and licensed
74 (Spanish patent number ES 2393728 A1, Barroso et al. 2014). Isolate CECT 2413 has
75 been demonstrated to be an effective *in vitro* antagonist against different isolates of *V.*

76 *dahliae*, as well as able to control VWO caused by the D pathotype under controlled
77 conditions and to promote olive growth (Barroso et al. 2014; Rincón et al. 2014).
78 Under specific conditions *V. dahliae* and *Trichoderma* spp. can develop resistant
79 structures, enabling them to survive under adverse conditions. Thus, *V. dahliae* produce
80 microsclerotia (MS), melanized structures mainly produced at the end of the parasitic
81 phase of its life's cycle and able to endure in soils for a prolonged period of time (Pegg
82 and Brady, 2002). On the other hand, many species of the genus *Trichoderma* develop
83 chlamydospores (globose or ellipsoidal, intercalary or terminal, smooth-walled,
84 yellowish, greenish or without colour, and with diameter between 6-15 μm) (Cohen et
85 al. 1983).
86 A key prerequisite to achieve effective biocontrol by any artificially-introduced
87 BCA is the efficient colonization of the target niche. The BCA must thus be able to
88 rapidly colonize the working site and to adapt and endure the harsh (a)biotic conditions
89 that they likely have to face after being released. However, this is not always the case
90 and there is an important lack of knowledge on the fate that a BCA undergoes after its
91 introduction in a new environment. A number of uncertainties still need to be tackled to
92 better understand why a BCA is not always able to behave in the way it is expected.
93 Regarding to the tripartite interaction olive-*Trichoderma*-*V. dahliae* nothing is known.
94 The specific objectives of this study were: (i) to study, at the microscopic level,
95 the interaction between *T. harzianum* CECT 2413 and *V. dahliae* D pathotype under *in*
96 *vitro* and *in planta* conditions; (ii) to determine the olive roots colonization process by
97 CECT 2413 over time; and (iii) to check whether isolate CECT 2413 is able to colonize
98 endophytically olive root tissues. We have aimed to better understand the behavior of
99 this BCA in the olive rhizosphere in the absence and presence of one of the most
100 devastating soil-borne pathogens affecting this woody crop.

101

102 **Materials and methods**

103 *Fungal isolates*

104 A green fluorescent protein (GFP)-labeled derivative of *T. harzianum* CECT 2413 (*Th*-

105 GFP; Chacón et al. 2007) and the enhanced yellow fluorescent protein (EYFP)-labeled

106 derivative of *V. dahliae* V937I D (isolate VDAT-36I; Prieto et al. 2009) were used in

107 this study. They were maintained at -80ºC and recovered when needed on potato

108 dextrose agar (PDA; Oxoid Ltd, Hampshire, UK).

109

110 In vitro *interaction of* Th-*GFP and VDAT-36I*

111 In order to examine the interaction between fluorescently-labeled derivatives of isolate

112 CECT 2413 and *V. dahliae* V937I, an experimental setup enabling microscopy

113 observation was designed. Sterile excavated microscope slides were prepared by filling

114 the concavities (15 mm diameter) with a thin layer of PDA. Then, both fungi were

115 deposited by gently touching with sterile toothpicks of which the tips were immersed in

116 saturated conidial suspensions of each fungus (*Th*-GFP and VDAT-36I). The distance

117 between both fungi was 1 cm (Fig. 1A). Slides were carefully deposited within sterile,

118 sealed Petri dishes and incubated during 72 h at 25ºC in the dark. The slides (5) were

119 observed by confocal laser scanning microscopy (CLSM) at 24, 48 and 72 h after

120 inoculation of the fungi with an Axioskop 2 MOT microscope (Carl Zeiss, Jena GmbH,

121 Germany) equipped with a Krypton and an Argon laser, controlled by Carl Zeiss Laser

122 Scanning System LSM5 PASCAL software (Carl Zeiss, Jena GmbH, Germany).

123 Enhanced *Th*-GFP was exposed to 488 nm Argon laser light (detection at 500-520 nm),

124 and the EYFP-labeled VDAT-36I to 514 nm Argon laser light (emission 530-620). The

125 same expositions were used for *in planta* tripartite interaction experiments (see below).

126 Data were recorded and the images transferred for analysis to Zeiss LSM Image
127 Browser version 4.0 (Carl Zeiss, Jena GmbH, Germany). Images were processed with
128 Photoshop CS6 (Adobe Systems Inc., San Jose, California, USA).
129
130 *Time course of early and long-term colonization events of olive roots by* T. harzianum
131 *CECT 2413*
132 A bioassay was performed with the aim to obtain detailed observations of the
133 colonization process in olive roots by the fluorescently-tagged derivative *Th*-GFP. A
134 single application of pre-germinated conidia of *Th*-GFP was performed using the
135 following procedure. Petri dishes containing PDA were inoculated with a mycelial disk
136 (5 mm diameter) and incubated at 25ºC in the dark during 5 days. Then, 5 ml of sterile
137 distilled water were added to each plate and the conidia were scraped and filtered by
138 sterile chiffon. This conidia suspension was used to inoculate Petri dishes of PDA (100
139 µl per plate). The plates were incubated until profuse conidiation (25ºC in the dark; 7
140 days), processed in the same way as described above to obtain the conidia suspension,
141 and quantified by using a haemocytometer. The inocula concentration was adjusted as
142 necessary. Conidia were germinated on potato dextrose broth (33%) (PDB; Oxoid Ltd,
143 Hampshire, UK) by incubating in an orbital shaker (200 rpm) during 15 h at 25ºC in the
144 dark. Conidia germination was corroborated by light microscope (Nikon YS100, Nikon
145 Corp., Tokyo, Japan) and the medium was eliminated by centrifugation (4400 rpm, 10
146 min; Eppendorf centrifuge 5804 R, Germany) and three washes with sterile distilled
147 water. Pre-germinated conidia were suspended in sterile distilled water and quantified
148 again using a haemocytometer. The experiment was conducted using 10-month olive
149 plants of the VWO susceptible cv. Picual (López-Escudero et al. 2004) originated from
150 a commercial nursery in Córdoba province (Southern Spain). The roots were carefully

151 washed under tap water avoiding intentional wounding, and dipped in a suspension of
152 $2x10^5$ *Th*-GFP pre-germinated conidia ml^{-1} prepared in minimal medium (MM) (Penttilä
153 et al. 1987) amended with 0.2% (w/v) glycerol as sole carbon source and 20 mg l^{-1} of
154 ammonium sulphate (Chacón et al. 2007). Plants with their root systems immersed in
155 this suspension were then placed in an orbital shaker (100 rpm) (Comecta SA 200-D, JP
156 Selecta Group, Barcelona, Spain) within a growth chamber at 24 ± 1ºC in the dark and
157 60-70 % relative humidity. After 12 h, the plants were transplanted to pots with
158 sterilized perlite and placed into a growth chamber with the same conditions described
159 above, but with a 14-h photoperiod of fluorescent light (360 mE m^{-2} s^{-1}) until the end of
160 the experiment (109 days). Plants were watered as needed, and fertilized weekly with 50
161 ml per pot of Nipofol-K Plus 12-4-36 + microelements (1 g l^{-1}) (Fercampo, Málaga,
162 Spain). For this experiment, 25 plants per treatment (i.e. un-inoculated control and *Th*-
163 GFP) were used. Microscope observations were performed 1, 2, 3, 7, 14, 21, 29, 90, 101
164 and 109 days after inoculation (DAI) collecting at least 2 plants per day. Samples
165 consisted in root segments (aprox. 1 cm long) carefully washed with sterile distilled
166 water. Longitudinal and transversal sections of root segments (50 µm width) were
167 obtained using a Vibratome (VT1000 S, Leica, Wetzlar, Germany). Additionally,
168 secondary roots were taken and visualized without tissue sectioning. Root sections were
169 stained with 10 µM propidium iodide (Sigma, Madrid, Spain) during 10 min to label the
170 plant cell walls. Samples from this bioassay were analyzed with a CLSM Microscope
171 (SP5 II, Leica, Wetzlar, Germany) using the LAS AF software (Leica Microsystems
172 Inc., Wetzlar, Germany). Images were processed with Photoshop CS6.
173
174 *Time course of interaction events of* Th-*GFP and VDAT-36I on olive roots*
175 For assessment of the pathogen-BCA-olive interaction, inoculations with *Th*-GFP,

176 VDAT-36I or *Th*-GFP+VDAT-36I were performed following the same procedure
177 described above for *T. harzianum* with some differences. Plant root systems were
178 dipped in MM modified as cited above containing 10^6 pre-germinated conidia ml^{-1} of
179 *Th*-GFP and placed in an orbital shaker (100 rpm) into a growth chamber (Percival SA
180 200-D, JP Selecta Group, Barcelona, Spain) at 24 ± 1ºC in the dark and 60-70 %
181 relative humidity. After 12 h, the plants were transferred into new containers with a
182 solution of MM modified with $5x10^6$ pre-germinated conidia ml^{-1} of VDAT-36I during
183 30 min. A group of control plants were only dipped in MM modified. Plants were then
184 transplanted to pots with sterilized soil (peat:sand:loan; 1:1:2) and placed into a growth
185 chamber with the same conditions described above but with a 14-h photoperiod with
186 fluorescent light (360 mE m^{-2} s^{-1}) until the end of the experiment (21 days). Plants were
187 watered as needed, and fertilized weekly. For this experiment, 18 plants per treatment
188 (i.e. un-inoculated control, *Th*-GFP, VDAT-36I and *Th*-GFP+VDAT-36I) were
189 inoculated.

190 Root tissue samples consisted in sections of about 1 cm length from the whole
191 root (one plant per treatment and per time-point), carefully washed with distilled water
192 to remove residual substrate. Microscope observations were performed 1, 2, 3, 7, 10, 14,
193 17 and 21 DAI and carried out using the CLSM cited previously for *in vitro* assay.
194 Images were also processed with Photoshop CS6.

195 Viability of *Th*-GFP was checked at the end of the experiment. Rhizosphere soil
196 was thus analyzed by using a *Trichoderma* selective medium (TSM) (Askew and Laing,
197 1993). Three replicate per plant and two plants per treatment were used. Colony
198 forming units (CFU) per g of soil were counted after incubation during 4 days at 25ºC in
199 the dark. Fluorescence of the colonies was checked using a Nikon Eclipse 80i
200 epifluorescence microscope (Nikon UK Ltd, Surrey, UK) to rule out that indigenous

201 *Trichoderma* spp. were present. Data means and standard deviations were calculated.

202

203 **Results**

204

205 In vitro *interaction between* Th-*GFP and VDAT-36I*

206 Dual cultures of the pathogen and *Th*-GFP performed on excavated microscopy slides

207 were prepared (Fig. 1a). CLSM observations performed at 24 h revealed that hyphae of

208 both fungi rapidly grew until they established contact and intermingled (Fig. 1b).

209 Evidence suggesting the existence of antibiosis was not found. Thereafter, events

210 associated with mycoparasitism were observed. Growth of *Th*-GFP over VDAT-36I

211 mycelium was observed at 72 h (Fig. 1a). CLSM imagery revealed that this overgrowth

212 was accompanied by numerous events of coiling (*Th*-GFP hyphae wrapping VDAT-36I

213 hyphae) (Fig. 1c-e; '*co*'). Other structures associated to this process such as papilla-like

214 (Fig. 1e; white arrowhead) or hook-like (Fig. 1e; red arrowhead) structures were

215 identified. Papilla-like structures consisted in growth and subsequence thickening of *Th*-

216 GFP vegetative hyphae alongside VDAT-36I hyphae, while hook-like structures were

217 identified in *Th*-GFP hyphae attached to *V. dahliae* hyphae as short lateral hyphal

218 branches. A loss of *Verticillium* mycelium fluorescence in that point was observed (Fig.

219 1e; red arrowhead). Furthermore, abundant asexual reproductive structures of both fungi

220 (i.e. conidia) were found (Fig. 1f; white and red arrows for *Th*-GFP and VDAT-36I,

221 respectively). On the contrary, *Th*-GFP chlamydospores (globose, smooth-walled with

222 an average diameter between 5.0-7.5 μm) were detected sporadically, mostly found at

223 the end of short lateral branches of vegetative hyphae (data not shown). Concerning

224 VDAT-36I, formation of MS was not observed during the experiment in contrast to the

225 high number of conidia detected (Fig. 1f; red arrows).

226

227 *Time course of early and long-term colonization events of olive roots by* Th-*GFP*

228 Visualization of *Th*-GFP biomass using CLSM was evident soon after artificial
229 inoculation of olive roots by the BCA. *Th*-GFP pre-germinated conidia were clearly
230 observed over the olive root surface one DAI (Fig. 2a; '*g*'). However, neither evidence
231 of penetration through the root epidermis nor preferential colonization sites were found
232 at this time point. As early as 2 DAI, first evidence of chlamydospore development was
233 obtained as revealed by appearance of slight hyphae swellings (Fig. 2b; yellow arrows).
234 Moreover, conidiophores were clearly visible as well (Fig. 2b; white asterisks).
235 Mycelium layers appeared profusely covering large surfaces of both principal and
236 secondary roots after three days (Fig. 2c). At this moment, conidia were also visualized
237 intermingled with mycelia and attached to the rhizoplane. First fully developed
238 chlamydospores also appeared at this time point (3 DAI) at both intercalary (Fig. 2c,
239 inset; white arrow) and distal positions (Fig. 2c, inset; red arrow). At 7 DAI showed
240 little or a total absence of fluorescent mycelium/hyphae. The vast majority of the *Th*-
241 GFP biomass visualized over the root surface, including root hairs, consisted of conidia
242 and chlamydospores firmly attached to the epidermis (Fig. 2d-e; '*c*' and '*ch*'). No major
243 changes were observed at 14 DAI compared to the previous time point: scarcity of
244 mycelium, high number of conidia attached to the root surface, and chlamydospores
245 differing neither in size nor in abundance over the rhizoplane (Fig. 2f-g; '*c*' and '*ch*').
246 At 21 DAI, chlamydospores were the most abundant fungal structure, covering large
247 areas of the olive root epidermis (Fig. 2h). Fluorescent hyphae were observed for the
248 last time in this experiment at this sampling time, although in very few spots (Fig. 2i;
249 '*h*'). No significant changes on appearance, abundance and distribution of *Th*-GFP
250 structures and biomass were observed over olive root surface at 29 DAI (Fig. 2j). From

251 this time point on, plants were kept under the same conditions to gain information about
252 the fate of *Th*-GFP biomass at long-term stages after inoculation (up to 100 DAI).
253 Chlamydospores were overwhelmingly observed at this late observation times (Fig 2k-l;
254 '*ch*'), although their number was very low. Bicellular chlamydospores were observed
255 (Fig 2k; black arrow) attached to epidermis. Morphology of chlamydospores in this
256 experiment did not differ to that generated during the *in vitro* experiment (i.e. globose
257 and smooth-walled) and their average diameters were around 10 µm. Overall, hyphae of
258 *Th*-GFP rapidly decreased over time and its biomass basically consisted of resistance
259 structures.
260

261 *Time course of early interaction events of Th-GFP and VDAT-36I on olive roots*

262 To visualize how *Th*-GFP and the pathogen colonize and interact on the olive root
263 system a similar approach was followed. A fair number of root tissue segments,
264 representative of the whole radical system of each sampled plant, were prepared on a
265 time-course basis and evaluated exhaustively by CLSM. At early stages (1 DAI), pre-
266 germinated conidia of both fungi were profusely detected over the root surface
267 regardless of whether or not fungi were single-inoculated (Fig. 3a and b; '*g*') or co-
268 inoculated (Fig. 3c; '*g*'). No preferential colonization site was observed. Noticeably, *Th*-
269 GFP started to develop both distal (Fig. 3a, white arrow; inset 1) and intercalary (Fig.
270 3a, red arrow; inset 2) chlamydospores very soon after inoculation. As observed in the
271 dual culture assay, chlamydospores were mainly found at terminal position. Overall,
272 few conidia were observed in this experiment for both fungi. At 2 DAI, most of the *Th*-
273 GFP biomass observed was in the form of chlamydospores, which profusely colonized
274 and covered entire zones of the rhizoplane regardless the absence (Fig. 3d; white
275 arrows) or presence (Fig. 3f; white arrows) of VDAT-36I. Whereas *Th*-GFP

276 chlamydospores increased over time, hyphae and conidia decreased dramatically.
277 Concerning the pathogen, its mycelium increased progressively as well, developing
278 aggregates of hyphae at specific spots on the root epidermis. These structures were
279 observed in both roots of plants inoculated only with VDAT-36I (Fig. 3e; '*ag*') and
280 with both fungi (Fig. 3f; '*ag*'). From 7 DAI on, fluorescent hyphae of both fungi
281 reduced drastically and were very difficult to observe, particularly for *Th*-GFP (Fig. 3g-
282 i). In contrast, massive development of chlamydospores was evident for *Th*-GFP (Fig.
283 3g and 3i; white arrows). Moreover, production of resistance structures (MS), evidenced
284 by hyphae aggregation and swelling, was observed for VDAT-36I over the root
285 epidermis (Fig. 3h-i; '*m*'). At later stages (10 DAI and on) neither fluorescent hyphae
286 nor conidia of *Th*-GFP were observed (Fig. 3j), and an overwhelming prevalence of
287 chlamydospores was revealed at some specific spots of the root surface (Fig. 3l; white
288 arrows). Regarding the pathogen, its biomass sharply decreased, being more difficult to
289 visualize except for scattered MS which tended to be the prevalent structure (Fig. 3k).
290 Overall, observation of fluorescent structures for both fungi was difficult at later days.
291 For instance, chlamydospores were the only structure detected at 14 DAI but they
292 usually lost fluorescence very fast. Thus, good quality CLSM images were not possible.
293 Eventually, at 17 and 21 DAI fluorescent fungal structures were not detected. No
294 evidence of endophytic colonization by *Th*-GFP was found along the bioassay.

295 Finally, quantification of viable *Th*-GFP propagules at the end of the experiment
296 yielded $1.5 \pm 0.4 \times 10^4$ and $4 \pm 0.7 \times 10^4$ cfu g^{-1} of soil in *Th*-GFP and *Th*-GFP+VDAT-
297 36I treatments, respectively. No indigenous *Trichoderma* spp. were recovered since all
298 grown colonies showed fluorescent under the fluorescence microscope. Likewise, no
299 *Trichoderma* spp. were detected in the rhizosphere of un-inoculated and VDAT-36I-
300 inoculated plants.

301

302 **Discussion**

303 The knowledge about the behavior of a given BCA when applied to the target niche
304 (ecology) and on the interactions established with the pathogen and the host plant
305 (trophic networks) is crucial for the successful application of BCA in agro-ecosystems.
306 In the present study, we have proved that *T. harzianum* CECT 2413 showed
307 mycoparasitism against *V. dahliae*, at least *in vitro*. Indeed, the typical events associated
308 to this process (Chet et al. 1998) were clearly observed. Mycoparasitism is considered
309 one of the main modes of action of *Trichoderma* spp. against fungal pathogens (e.g.
310 Druzhinina et al. 2011). Chet et al. (1998) described four crucial steps during
311 mycoparasitism: (1) chemotropism, (2) recognition, (3) attachment and coiling, and (4)
312 lytic activity leading to death of the mycelium. In our *in vitro* experimental setup, the
313 attachment, characterized by hyphal growth alongside the pathogen hyphae and
314 appearance of specialized structures (i.e. papillae and hooks), and coiling previous to
315 pathogen mycelial degradation were undoubtedly visualized. Papilla-like structures of
316 *Trichoderma* spp. have been defined previously for other pathosystems (Lu et al. 2004;
317 Druzhinina et al. 2011). These structures are similar to those reported in cucumber
318 (Yedidia et al. 2000) and tomato roots (Chacón et al. 2007), identified as appressoria-
319 like structures and analogous to the appresorium of plant pathogens (Druzhinina et al.
320 2011). Furthermore, *Trichoderma* can grow upon the prey and develop parasitic
321 interactions developing hook-shape structures that are also involved in penetrating the
322 host’s mycelium by physical or chemical mechanisms (Lu et al. 2004; Brotman et al.
323 2010). Nonetheless, among all morphological features observed during the
324 mycoparasitic interaction in *Trichoderma* spp., coiling is the most noteworthy. The
325 capability of forming helix-shape hyphae around the pathogen, also present in other

326 pathosystems (e.g. Lu et al. 2004), can also be key for a successful biological control
327 effect. In the present study, these structures were observed clearly *in vitro*, wrapping *V.*
328 *dahliae* hyphae. These microscopic events coincided with *V. dahliae* overgrowth by
329 CECT 2413, an event usually associated with other mycoparasitic events (e.g.
330 Ghanbarzadeh et al. 2014). However, there was no evidence of mycoparasitism in our *in*
331 *planta* experiment, although we cannot completely rule out its occurrence on olive
332 roots, nor exclude the presence of additional mechanisms among the battery of weapons
333 this biocontrol fungus may deploy (Benítez et al. 2004). Chet et al. (1998) argued that
334 parasitic interactions occur with less intensity *in planta* than in dual cultures due to a
335 low nutrient concentration in soil if compared with the media.

336 The root colonization process by isolate CECT 2413, previously documented for
337 herbaceous species (Chacón et al. 2007; Samolski et al. 2012; Alonso-Ramírez et al.
338 2014), has been elucidated here for olive. In this woody plant, CECT 2413 showed a
339 high root colonization capability, as otherwise demonstrated for different isolates of
340 *Trichoderma* spp. (Lu et al. 2004; Hohmann et al. 2011). Furthermore, *Th*-GFP was
341 observed in the same spots as the pathogen. This fact could be essential for the success
342 of biocontrol, as suggested by Kato et al. (2012). *Trichoderma* spp. are traditionally
343 considered as fungi with high saprophytic and epiphytic activities, although usually
344 limited to superficial layers when colonizing plant roots. Nevertheless, in some cases
345 they can gain entrance to the plant interior (Harman et al. 2004). Endophytic lifestyle
346 has thus been shown for several *Trichoderma* spp. isolates (Lu et al. 2004; Chacon et al.
347 2007; Hohmann et al. 2012). Unlike in the above-mentioned studies with herbaceous
348 plants, there was no evidence for olive inner root colonization by CECT 2413.

349 In this study, CECT 2413 was inoculated as (pre-germinated) conidia
350 suspensions. Hence, these structures were observed abundantly at early stages after

351 inoculation. Furthermore, development of conidiophores was also observed *in planta*
352 during the first sampling time points. However, both conidia and conidiophores
353 gradually disappeared at later observation times, as previously reported (Bae and
354 Knudsen 2000). This could be explained due to the fact that conidia can be highly
355 sensitive to soil fungistasis (Papavizas 1985). Overall, conidia usually show lower
356 survival rate under natural conditions compared with other asexual propagules (Lewis
357 and Papavizas 1983). Conidia were not the only propagule identified during the
358 bioassays. Indeed, CECT 2413 developed a large number of chlamydospores. These
359 resistant structures, previously identified/named as "yeast-like cells" by others (Chacón
360 et al. 2007; Alonso-Ramírez et al. 2014), have been described for *Trichoderma* spp. in
361 several environments such as liquid and solid media (Lewis and Papavizas 1983) or
362 sterile natural and artificial soils (Park 1954). Papavizas et al. (1985) suggested that
363 production of chlamydospores can be related to a survival strategy of the fungus when
364 introduced in natural ecosystems. The prevalence of resistance structures of
365 *Trichoderma* could then be explained by nutrient shortage in the rhizosphere and the
366 subsequent slow down of the BCA metabolism. Furthermore, Cohen et al. (1983)
367 suggested that presence of organic/living matter such as plant tissues could favor
368 chlamydospore formation and survival in soil. Thus, the overwhelming abundance of
369 this resistant structure observed in our bioassays may be a consequence either of a
370 normal behavior of this BCA in this particular niche or to a survival strategy due to
371 adverse environmental conditions. So far, we do not have evidences supporting any of
372 these two alternatives. Interestingly, chlamydospore formation took place under
373 presence/absence of the pathogen. The production of an increasing number of
374 chlamydospores on olive roots was concomitant with the progressive decrease of
375 fluorescent hyphae that either eventually showed a substantial reduction (*viz. Th*-olive

376 experiment) or a total absence at late observation times (*viz. Th*-olive-VDAT-36I
377 experiment). While *Th*-GFP seemed to be absent at 17 DAI (no detectable fluorescent
378 structures), viable CECT 2413 propagules were still present at the end of the *Th*-olive-
379 VDAT-36I experiment as demonstrated by TSM quantification, although the BCA
380 population size had decreased by two orders of magnitude regarding to the initial
381 inoculum density. This fact together with the presence of chlamydospores after more
382 than 100 days in *Th*-olive experiment confirmed the presence of this BCA in the olive
383 rhizosphere, predominantly as resistant structure though. Therefore, we suggest a
384 dormant state of the fungus in the form of chlamydospores in our experiments rather
385 than loss of the inoculum. The way in which the BCA is applied can therefore
386 determine its success in exerting biocontrol. Thus, when they are inoculated as conidia,
387 chlamydospores or even at early conidia germination stages, their performance could be
388 diminished because of the lack of nutrient sources. The likelihood of success would be
389 enhanced when an adequate nutrients supply is added to the inocula (Yang et al. 2011).
390 Pertot et al. (2008) stressed the importance that an adequate survival rate has for a
391 successful biocontrol activity. The use of appropriate carriers is therefore a crucial
392 factor when formulating and delivering BCA into a new environment. In this way,
393 problems of inactivation, death and/or loss of biocontrol effectiveness of the BCA could
394 be overcome (El-Hassan and Gowen 2006). Additionally, a regular supply of the BCA
395 to maintain an adequate population level in the target niche could also be needed to
396 counteract inoculum loss (Knudsen et al. 1991).
397 Few studies about the interaction of biocontrol fungi in plant roots by using
398 advanced microscopy approaches are available (for instance, Zachow et al. 2010 and
399 Kato et al. 2012). Recently, Lace et al. (2015) analysed, under *in vitro* culture
400 conditions, the interactions between *Trichoderma atroviride* PKI1, two *Gigaspora*

401 species and the herbaceous plant *Medicago truncatula* Gaertn. The same *Trichoderma*
402 isolate used in the present study has been used in herbaceous species as well (Chacón et
403 al. 2007; Samolski et al. 2012; Alonso-Ramírez et al. 2014). However, to the best of our
404 knowledge, our work is the first one addressing the long-term colonization process of
405 this BCA in a woody plant rhizosphere by CLSM that is, using living tissue. Moreover,
406 we have been able to unravel the fate of the BCA biomass in this dynamic ecological
407 niche over a long period of time, in the presence and absence of the target
408 phytopathogen and under non-gnotobiotic conditions. Events here reported provide
409 essential information (i.e. prevalence of chlamydospores) about the behavior of this
410 BCA which can help to design more effective *Trichoderma*-based bioformulations.
411 These bioformulations should be based on adequate carriers ensuring not only the
412 activity of the BCA but also its durability.
413

414 **References**

415 Aleandri MP, Chilosi G, Bruni N, Tomassini A, Vettraino AM, Vannini A (2015) Use of
416 nursery potting mixes amended with local *Trichoderma* strains with multiple
417 complementary mechanisms to control soil-borne diseases. Crop Prot 67:269-278
418 Alonso-Ramirez A, Poveda J, Martin I, Hermosa R, Monte E, Nicolas C (2014) Salicylic acid
419 prevents *Trichoderma harzianum* from entering the vascular system of roots. Mol Plant
420 Pathol 15(8):823-831
421 Askew DJ, Laing MD (1993) An adapted selective medium for the quantitative isolation of
422 *Trichoderma* species. Plant Pathol 42(5):686-690
423 Bae YS, Knudsen GR (2000) Cotransformation of *Trichoderma harzianum* with beta-
424 glucuronidase and green fluorescent protein genes provides a useful tool for monitoring
425 fungal growth and activity in natural soils. Appl Environ Microbiol 66(2):810-815

426 Barroso Albarracín JB, Carreras Egaña A, Valderrama Rodríguez R, Chaki M, Begara Morales
427 J, Mercado-Blanco J, Pérez Artés E, Rincón Romero A, Carballo Codón A, Benítez
428 Fernández T, Valverde Corredor A, Guevara Pezoa F, Rodríguez Palero MJ, Dueñas
429 Sánchez R, Fierro Risco J, López García A (2014) Cepa de *Trichoderma* útil para el
430 tratamiento y/o prevención de infecciones provocadas por hongos pertenecientes al
431 género *Verticilium*. Spanish Patent ES2393728
432 Benítez T, Rincón AM, Limón MC, Codón AC (2004) Biocontrol mechanisms of *Trichoderma*
433 strains. Int Microbiol 7:249–260
434 Brotman Y, Kapuganti JG, Viterbo A (2010) *Trichoderma*. Curr Biol 20 (9):R390-R391
435 Carvalho DDC, Lobo M, Martins I, Inglis PW, Mello SCM (2014) Biological control of
436 *Fusarium oxysporum* f. sp *phaseoli* by *Trichoderma harzianum* and its use for common
437 bean seed treatment. Trop Plant Pathol 39(5):384-391
438 Chacón MR, Rodríguez-Galán O, Benítez T, Sousa S, Rey M, Llobell A, Delgado-Jarana J
439 (2007) Microscopic and transcriptome analyses of early colonization of tomato roots by
440 *Trichoderma harzianum*. Int Microbiol 10(1):19-27
441 Chet I, Benhamou N, Haran S (1998) Mycoparasitism and lytic enzymes. In: Harman GE,
442 Kubicek CP (eds) *Trichoderma* & *Gliocladium*. Enzymes, biological control and
443 commercial applications, vol 2. Taylor and Francis Ltd, United Kingdom, pp 153-172
444 Cohen SD, Lewis JA, Papavizas GC, Bean GA (1983) Chlamydospore formation by
445 *Trichoderma* spp. in organic-matter amended soil. Phytopathology 73(5):820 (Abstract
446 A428)
447 Contreras-Cornejo HA, Ortiz-Castro R, López-Bucio J (2013) Promotion of plant growth and
448 the induction of systemic defence by *Trichoderma*: physiology, genetics and gene
449 expression. In: Mukherjee PK, Horwitz BA, Singh US, Mukherjee M, Schmoll M (eds)
450 *Trichoderma*: biology and applications. CABI, Walingford, UK, pp 173-194

451 Druzhinina IS, Seidl-Seiboth V, Herrera-Estrella A, Horwitz BA, Kenerley CM, Monte E,
452 Mukherjee PK, Zeilinger S, Grigoriev IV, Kubicek CP (2011) *Trichoderma*: The
453 genomics of opportunistic success. Nat Rev Microbiol 9(10):749-759
454 El-Hassan SA, Gowen SR (2006) Formulation and delivery of the bacterial antagonist *Bacillus*
455 *subtilis* for management of lentil vascular wilt caused by *Fusarium oxysporum* f. sp
456 *lentis*. J Phytopathol 154(3):148-155
457 Ghanbarzadeh B, Safaie N, Goltapeh EM (2014) Antagonistic activity and hyphal interactions
458 of *Trichoderma* spp. against *Fusarium proliferatum* and *F. oxysporum in vitro*. Arch
459 Phytopathol Plant Prot 47(16):1979-1987
460 Harman GE, Howell CR, Viterbo A, Chet I, Lorito M (2004) *Trichoderma* species -
461 Opportunistic, avirulent plant symbionts. Nat Rev Microbiol 2(1):43-56
462 Harman GE, Kubicek CP (1998) *Trichoderma* & *Gliocladium*. Vol. 2. Enzymes, biological
463 control and commercial applications, vol 2. Taylor & Francis Ltd, United Kingdom
464 Hermosa R, Viterbo A, Chet I, Monte E (2012) Plant-beneficial effects of *Trichoderma* and of
465 its genes. Microbiology-(UK) 158:17-25
466 Hohmann P, Jones EE, Hill RA, Stewart A (2011) Understanding *Trichoderma* in the root
467 system of *Pinus radiata*: associations between rhizosphere colonisation and growth
468 promotion for commercially grown seedlings. Fungal Biol 115(8):759-767
469 Hohmann P, Jones EE, Hill RA, Stewart A (2012) Ecological studies of the bio-inoculant
470 *Trichoderma hamatum* LU592 in the root system of *Pinus radiata*. FEMS Microbiol
471 Ecol 80(3):709-721
472 Jiménez-Díaz RM, Trapero-Casas JL, Boned J, Landa del Castillo BB, Navas-Cortés JA (2009)
473 Uso de Bioten para la protección biológica de plantones de olivo contra la Verticilosis
474 causada por el patotipo defoliante de *Verticillium dahliae*. Bol. San. Veg. Plagas,
475 35:595-615 (with an abstract in English)

476 Kato A, Miyake T, Nishigata K, Tateishi H, Teraoka T, Arie T (2012) Use of fluorescent
477 proteins to visualize interactions between the Bakanae disease pathogen *Gibberella*
478 *fujikuroi* and the biocontrol agent *Talaromyces* sp KNB-422. J Gen Plant Pathol
479 78(1):54-61
480 Knudsen GR, Eschen DJ, Dandurand LM, Bin L (1991) Potential for biocontrol of *Sclerotinia*
481 *sclerotiorum* through colonization of sclerotia by *Trichoderma harzianum*. Plant
482 Disease 75:466-470
483 Kredics L, Hatvani L, Naeimi S, Körmöczi P, Manczinger L, Vágvölgyi C, Druzhinina I (2014)
484 Chapter 1 - Biodiversity of the genus *Hypocrea/Trichoderma* in different habitats. In:
485 Gupta VK, Schmoll M, Herrera-Estrella A, Upadhyay RS, Druzhinina I, Tuohy M (eds)
486 Biotechnology and Biology of *Trichoderma*. Elsevier, Amsterdam, pp 3-24
487 Lace B, Genre A, Woo S, Faccio A, Lorito M, Bonfante P (2015) Gate crashing arbuscular
488 mycorrhizas: *In vivo* imaging shows the extensive colonization of both symbionts by
489 *Trichoderma atroviride*. Env Microbiol Rep 7(1):64-77
490 Lewis JA, Papavizas GC (1983) Production of chlamydospores and conidia by *Trichoderma*
491 spp in liquid and solid growth media. Soil Biol Biochem 15(3):351-357
492 López-Escudero FJ, del Río C, Caballero JM, Blanco-López MA (2004) Evaluation of olive
493 cultivars for resistance to *Verticillium dahliae*. Eur J Plant Pathol 110(1):79-85
494 López-Escudero FJ, Mercado-Blanco J (2011) Verticillium wilt of olive: A case study to
495 implement an integrated strategy to control a soil-borne pathogen. Plant Soil 344(1):1-
496 50
497 Lorito M, Woo S (2015) *Trichoderma*: A multi-purpose tool for integrated pest management.
498 In: Lugtenberg B (ed) Principles of Plan-Microbe Interactions. Microbes for Sustainable
499 Agriculture. Springer, Switzerland, pp 345-353
500 Lu ZX, Tombolini R, Woo S, Zeilinger S, Lorito M, Jansson JK (2004) *In vivo* study of

501 *Trichoderma*-pathogen-plant interactions, using constitutive and inducible green
502 fluorescent protein reporter systems. Appl Environ Microbiol 70(5):3073-3081
503 Mercado-Blanco J, Rodríguez-Jurado D, Hervás A, Jiménez-Diaz RM (2004) Suppression of
504 Verticillium wilt in olive planting stocks by root-associated fluorescent *Pseudomonas*
505 spp. Biol Control 30(2):474-486
506 Moreno-Mateos MA, Delgado-Jarana J, Codón AC, Benítez T (2007) pH and Pac1 control
507 development and antifungal activity in *Trichoderma harzianum*. Fungal Genet Biol
508 44(12):1355-1367
509 Papasotiriou FG, Varypatakis KG, Christofi N, Tjamos SE, Paplomatas EJ (2013) Olive mill
510 wastes: A source of resistance for plants against *Verticillium dahliae* and a reservoir of
511 biocontrol agents. Biol Control 67(1):51-60
512 Papavizas GC (1985) *Trichoderma* and *Gliocladium*- Biology, ecology, and potential for
513 biocontrol. Annu Rev Phytopathol 23:23-54
514 Park D (1954) Chlamydospores and survival in soil fungi. Nature 173:454-455
515 Pegg GF, Brady BL (2002) Verticillium wilts. CAB International, Wallingford
516 Penttilä M, Nevalainen H, Rättö M, Salminen E, Knowles J (1987) A versatile transformation
517 system for the cellulolytic filamentous fungus *Trichoderma reesei*. Gene 61(2):155-164
518 Pertot I, Gobbin D, De Luca F, Prodorutti D (2008) Methods of assessing the incidence of
519 Armillaria root rot across viticultural areas and the pathogen's genetic diversity and
520 spatial–temporal pattern in northern Italy. Crop Prot 27(7):1061-1070
521 Prieto P, Navarro-Raya C, Valverde-Corredor A, Amyotte SG, Dobinson KF, Mercado-Blanco
522 J (2009) Colonization process of olive tissues by *Verticillium dahliae* and its in planta
523 interaction with the biocontrol root endophyte *Pseudomonas fluorescens* PICF7. Microb
524 Biotechnol 2(4):499-511
525 Raaijmakers JM, Paulitz TC, Steinberg C, Alabouvette C, Moenne-Loccoz Y (2009) The

526 rhizosphere: a playground and battlefield for soilborne pathogens and beneficial
527 microorganisms. Plant Soil 321(1-2):341-361
528 Rincón AM, Chaki M, Fierro-Risco J, Valverde-Corredor A, Carreras A, Pérez-Artés E, Begara
529 JC, Valderrama R, Barroso JB, Mercado-Blanco J (2014) Biological control of
530 Verticillium wilt of olive by *Trichoderma harzianum*. In: XII Meeting of the
531 IOBC/wprs Working Group "Biological control of fungi and bacterial plant pathogens".
532 Upsala, Sweden, p 78
533 Ruano-Rosa D, Cazorla FM, Bonilla N, Martín-Pérez R, De Vicente A, López-Herrera CJ
534 (2014) Biological control of avocado white root rot with combined applications of
535 *Trichoderma* spp. and rhizobacteria. Eur J Plant Pathol 138(4):751-762
536 Ruano-Rosa D, del Moral-Navarrete L, Lopez-Herrera CJ (2010) Selection of *Trichoderma*
537 spp. isolates antagonistic to *Rosellinia necatrix*. Span J Agric Res 8(4):1084-1097
538 Samolski I, Rincón AM, Pinzón LM, Viterbo A, Monte E (2012) The qid74 gene from
539 *Trichoderma harzianum* has a role in root architecture and plant biofertilization.
540 Microbiol-SGM 158(1):129-138
541 Tjamos EC (1993) Prospects and strategies in controlling Verticillium wilt of olive. EPPO
542 Bulletin 23(3):505-512
543 Verma M, Brar SK, Tyagi RD, Surampalli RY, Valéro JR (2007) Antagonistic fungi,
544 *Trichoderma* spp.: Panoply of biological control. Biochem Eng J 37(1):1-20
545 Vitullo D, Altieri R, Esposito A, Nigro F, Ferrara M, Alfano G, Ranalli G, De Cicco V, Lima G
546 (2013) Suppressive biomasses and antagonist bacteria for an eco-compatible control of
547 *Verticillium dahliae* on nursery-grown olive plants. Int J Environ Sci Technol
548 10(2):209-220
549 Yang XM, Chen LH, Yong XY, Shen QR (2011) Formulations can affect rhizosphere
550 colonization and biocontrol efficiency of *Trichoderma harzianum* SQR-T037 against

551 Fusarium wilt of cucumbers. Biol Fertil Soils 47(3):239-248

552 Yedidia I, Benhamou N, Kapulnik Y, Chet I (2000) Induction and accumulation of PR proteins
553 activity during early stages of root colonization by the mycoparasite *Trichoderma*
554 *harzianum* strain T-203. Plant Physiol Biochem 38(11):863-873

555 Zachow C, Fatehi J, Cardinale M, Tilcher R, Berg G (2010) Strain-specific colonization pattern
556 of *Rhizoctonia* antagonists in the root system of sugar beet. FEMS Microbiol Ecol
557 74(1):124-135

558

559 **Figure captions**

560 **Fig. 1** *In vitro* analysis of the interaction between fluorescently-labeled derivatives of
561 *Trichoderma harzianum* CECT 2413 (*Th*-GFP) and a defoliating representative of the
562 soil-borne pathogen *Verticillium dahliae* (VDAT-36I) using confocal laser scanning
563 microscopy. Dual cultures were incubated (25ºC, 72 h) in excavated microscope slides
564 filled in with potato-dextrose-agar medium. **a**, Macroscopic view of the experimental
565 setup 72 h after inoculation. Fungi were inoculated at a distance of 1 cm. **b**,
566 Intermingled growth of *Th*-GFP (green) and VDAT-36I (yellow) hyphae observed at 48
567 h after inoculation. **c**-**e**, Hyphae of *Th*-GFP (green) forming coils wrapping VDAT-36I
568 hyphae (yellow) observed at 72 h. Papilla-like (white arrowhead) and hook-like (red
569 arrowhead) structures were observed together with degradation of VDAT-36I mycelia
570 (red arrowhead). Panel **d** shows the inset indicated by a dashed-line square in panel **c**. **f**,
571 Asexual reproductive structures of *Th*-GFP (white arrows) and VDAT-36I (red arrows).
572 Bars represent 10 μm in all panels except in **b** where it represents 50 μm. (*co*) coiling

573

574 **Fig. 2** *In vivo* confocal laser scanning microscopy analysis of olive (cv. Picual) roots
575 colonization by a GFP-labeled *Trichoderma harzianum* CECT 2413 (*Th*-GFP). Three

576 types of root tissue samples were used: longitudinal (**a**-**b**, **d**-**f**, **i**-**l**) and transversal (**g**)
577 vibratome sections (50 µm width), and secondary roots without sectioning (**c**, **h**). All
578 samples were stained with 10 µM Propidium-iodide. **a**, Pre-germinated conidia and
579 hyphal growth on root surface one day after inoculation (DAI). **b**, Hyphal growth two
580 DAI where first evidences of chlamydospore development appears as hyphal swelling
581 (yellow arrows). Asterisks indicate conidiophores, asexual reproduction structures. **c**,
582 Hyphae are observed covering large portions of the root surface at three DAI. First
583 chlamydospores are observed in terminal and intercalary positions (inset: red and white
584 arrows, respectively). **d**-**e**, chlamydospores appear as the predominant fungal structure
585 on the root surface at seven DAI. Conidia still appear in large number while hyphae
586 begin to disappear. **f**-**g**, at 14 DAI Conidia and chlamydospores of *Th*-GFP were found
587 surrounding root hairs. **h**-**i**, Extensive colonization of the root surface after 21 DAI,
588 mainly as conidia and chlamydospores. Progressive loss of hyphae fluorescence was
589 observed. **j**, Prevalence of chlamydospores and conidia after 29 DAI with complete
590 absence of fluorescent hyphae. **k**-**l**, Chlamydospores and conidia, but no fluorescent
591 hyphae in the rhizoplane at 101 DAI. Black arrow (**k**) points to a chlamydospore with
592 two cells. Bars represent 10 µm in panels **g** and **k**, 30 µm in **a**, **b**, **d**, **e**, **f**, **i**, **j** and **l**, 100
593 µm in **c** and **h**. (*c*) conidia; (*ch*) chlamydospore; (*g*) germinated conidia; (*h*) hyphae; (*r*)
594 root; (*rh*) root hair
595
596 **Fig. 3** *In planta* interaction between *Trichoderma harzianum* CECT 2413 and
597 *Verticillium dahliae* VDAT36I. Confocal laser scanning microscopy images showing
598 the time-course of *in planta* colonization of olive (cv. Picual) roots of *Trichoderma*
599 *harzianum* CECT 2413 (*Th*-GFP, green, left panels column), *Verticillium dahliae*
600 VDAT36I (dark yellow, central panels column), and both fungi together (right panels

601 column). Images show representative samples of the whole root system sampled at one
602 (**a**-**c**), two (**d**-**f**), seven (**g**-**i**) and ten (**j**-**l**) days after inoculation. **a**, Conidia and hyphae of
603 *Th*-GFP colonizing the olive root epidermis. Development of distal (white arrow; inset
604 **a1**) and intercalary (red arrows; inset **a2**) chlamydospores. **b**, Conidia germination and
605 hyphal growth of VDAT-36I on root surface. **c**, Root surface showing little presence of
606 *Th*-GFP chlamydospore. **d**, Increasing number of chlamydospores face to an important
607 decrease of conidia and hyphae. **e**, Accumulation of VDAT-36I hyphae in root surface
608 following a random pattern. **f**, *Th*-GFP and VDAT-36I on root surface with profuse
609 colonization by both fungi sharing the same spot. After this moment, hyphae of *Th*-GFP
610 were no longer detected. **g**, Chlamydospores around root hairs. A low number of
611 conidia and complete absence of hyphae were observed. **h**, VDAT-36I starts to develop
612 microsclerotia. Presence of hyphae was scarce. **i**, *Th*-GFP chlamydospores and VDAT-
613 36I microsclerotia on root surface. Both fungi are occupying the same spot. After this
614 moment, VDAT-36I hyphae were no longer detected. **j**, Chlamydospores covering
615 regions of the rhizoplane. **k**, Microsclerotium. **l**, High number of *Th*-GFP
616 chlamydospores covering large regions of the root surface. Bars represent 50 µm in all
617 panels except in **a1** and **a2** where represent 10 µm. (*ag*) aggregate; (*c*) conidia; (*g*)
618 germinated conidia; (*h*) hypha; (*m*) microsclerotia; (*r*) root; (*rh*) root hair; 'white and
619 red arrows' indicate chlamydospores

Acknowledgments

We are very grateful to M. N. Casa Adán for the help with CLSM at the University of Jaén facilities, and to M. Maldonado-González and A. Valverde-Corredor for their technical assistance. We appreciate the collaboration of NUTESCA SL in this project. This work was supported by European Regional Development Fund-cofinanced grants from the Spanish Ministry of Economy and Competitiveness [project number BIO2012-33904] and 'Junta de Andalucía' [project number AGR-6038].

colour figure

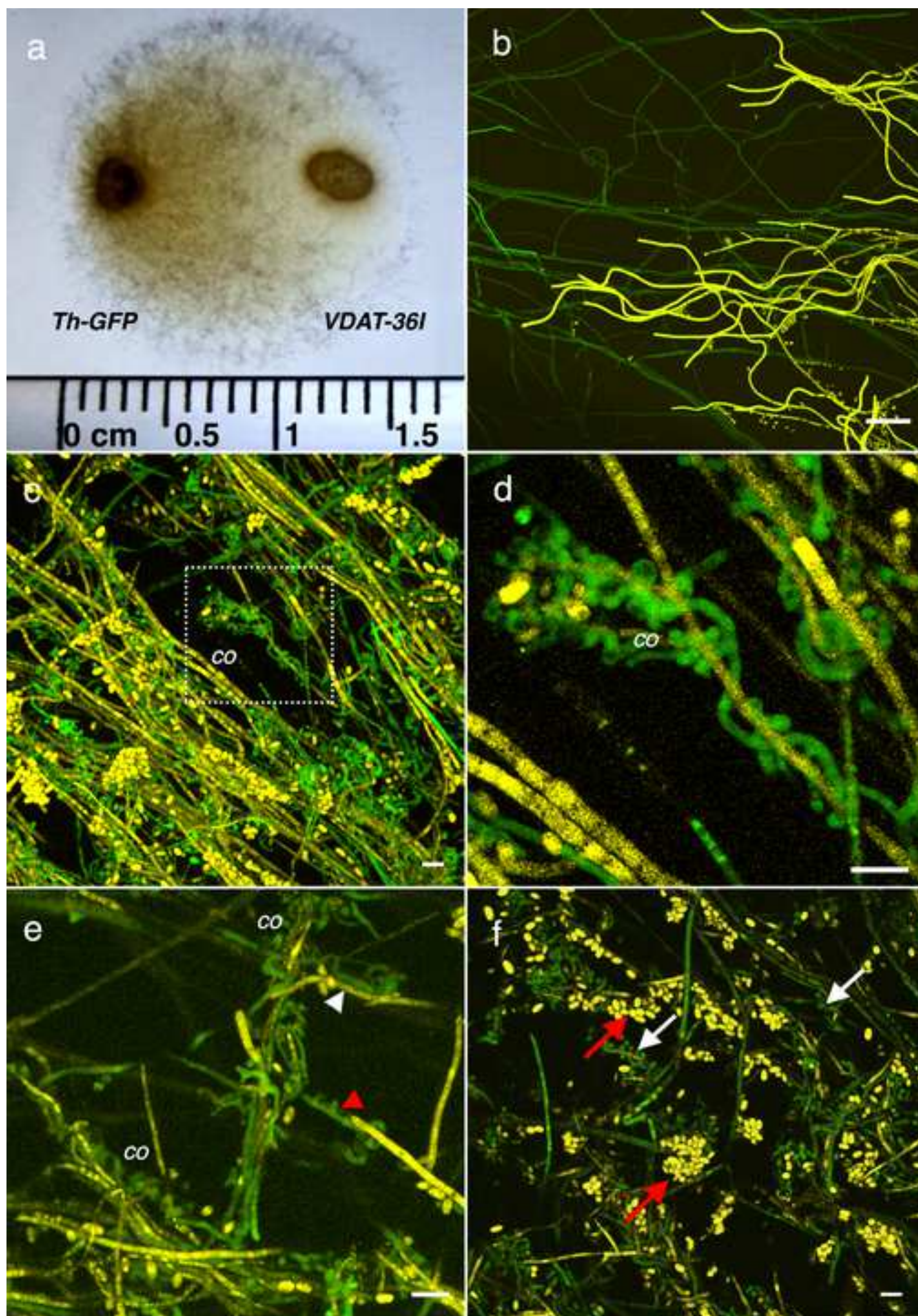

colour figure

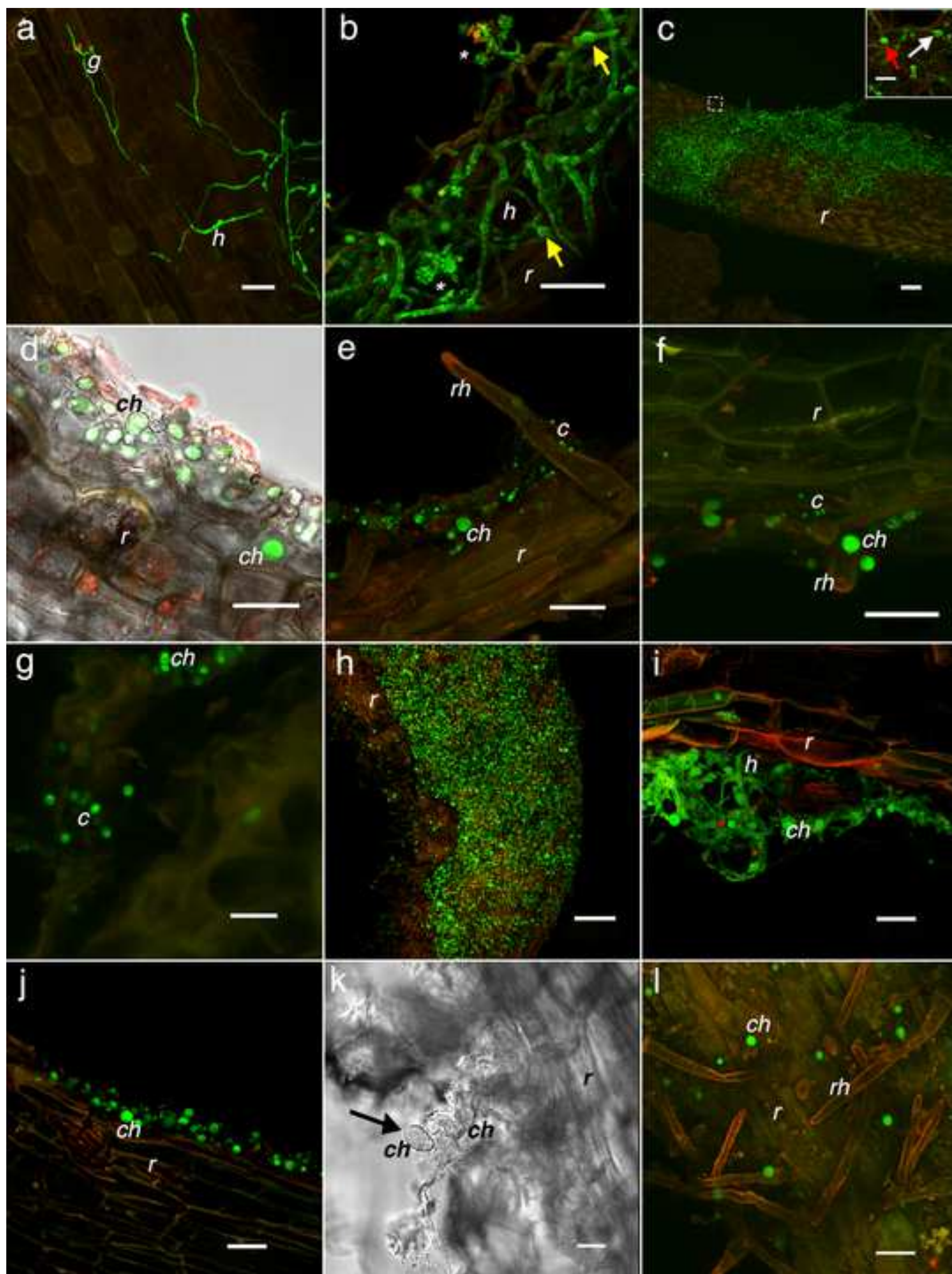

colour figure